First Demonstration of a 10-Gb/s RZ End-to-End Four-Wave-Mixing Based Link at 1884 nm Using Silicon Nanowaveguides

Noam Ophir, *Student Member, IEEE*, Ryan K. W. Lau, *Student Member, IEEE*, Michaël Ménard, *Member, IEEE*, Reza Salem, *Member, IEEE*, Kishore Padmaraju, *Student Member, IEEE*, Yoshitomo Okawachi, *Senior Member, IEEE*, Michal Lipson, *Senior Member, IEEE*, Alexander L. Gaeta, *Fellow, IEEE*, and Keren Bergman, *Fellow, IEEE*

Abstract—We demonstrate a double-stage four-wave mixing (FWM) scheme in silicon nanowaveguides which allows effective optical time-division-multiplexed data generation and reception in the 2-μm region. The scheme is based on a first mixing stage which unicasts a high-speed return-to-zero stream from the C-band to 1884-nm, followed by a second mixing stage which wavelength converts the data from 1884-nm down to the O-band for detection. The 10-Gb/s data traverses an aggregate record distance of 909 nm in the cascaded wavelength-conversion and unicast stages, with a power penalty of 2.5 dB. This scheme effectively overcomes the lack of commercially-available high-performance sources and receivers at 2 μm by relying on telecommunication band components along with ultrabroad FWM silicon devices.

Index Terms—Optical frequency conversion, optical Kerr effect, optical signal processing, silicon-on-insulator technology.

I. Introduction

THE EXPONENTIAL growth of network traffic witnessed in recent years at constant pace of 60% per year [1] requires the introduction of new optical communication technologies if telecom is to continue sustaining this growth. Most recent approaches to increase the optical communication

bandwidth, with demonstrations exceeding 100 Tb/s [2]–[5], have focused on utilizing advanced modulation formats and massive wavelength parallelism within the telecom bands as well as spatial parallelism using multi-core fibers. While these techniques enable a significant increase to link bandwidth, the growing data bandwidth demands might require even greater scaling of optical links capacity.

An additional complementary approach to increase system capacity is to attempt to utilize a broader 1.2-2 μm communication spectrum. Optical gain elements such as rare-earth doped fiber amplifiers, semiconductor optical amplifiers (SOAs), parametric amplifiers, and Raman amplifiers [6]–[9] can potentially enable operation outside the telecom bands. Light sources and receivers are also available at such wavelengths but device performance is still significantly lower compared to standard telecom devices. This performance gap can potentially be bridged by introducing ultra-broad phase-preserving wavelength converters which can translate signals to and from the telecom bands, effectively exporting capabilities into other wavelength bands.

Dispersion engineering of silicon waveguides has enabled four-wave mixing (FWM)-based optical processing at record Tbaud/s symbol rates and broad continuous phase-matched wavelength-conversion bandwidth across hundreds of nanometers [10]–[12]. Furthermore, complementary metal-oxide-semiconductor (CMOS)-compatible silicon waveguides present a well-refined mass-producible platform for optical nonlinear processing, requiring relatively simple fabrication and allowing for dense integration with microelectronics.

In this manuscript we report the first demonstration of data conversion from the telecom bands to the 2-μm region and back in silicon using a double-stage FWM setup. One chip converts 10-Gb/s return-to-zero (RZ) data from 1546.8 nm to 1884 nm using a unicast functionality (data modulated on a FWM pump) followed by a second chip in which the data signal is wavelength converted (data modulated on probe) from 1884 nm to 1312 nm. We validate system performance by bit-error-rate (BER) measurements on both stages, showing a power penalty (measured at a BER of 10^{-9}) of 0.4 dB from the first stage, a total 2.5 dB for both stages combined, and observe error free operation (BER $<10^{-12}$) of all signals. At
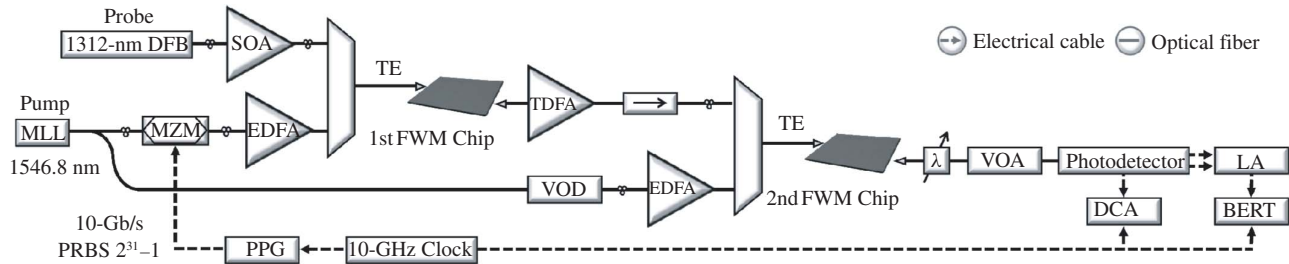
Fig. 1. Experimental setup of the double-stage FWM experiment. The first FWM chip performs a unicast from 1546.8 to 1884 nm. The second chip performs a wavelength conversion from 1884 to 1312 nm.

909 nm aggregate conversion, this is the largest wavelength conversion of data in silicon reported to date.

II. DEVICES, EXPERIMENTS, AND RESULTS

The FWM nanowaveguides were fabricated at the Cornell Nanofabrication Facility using e-beam lithography followed by reactive ion etching. The oxide-clad nanowaveguides are 1.1 cm long with a 300-nm by 710-nm cross section surrounded by a 30-nm slab. Device dimensions were optimized for quasi-TE operation with a zero-group-velocity dispersion (ZGVD) wavelength in the C-band. We estimated the ZGVD wavelength to be 1546.5 nm by optimizing the pump position to yield maximal wavelength-conversion bandwidth. Inverse tapers on both facets provide efficient coupling to fiber. Both devices are laid out in compact spirals occupying less than 1 mm^2. The fiber-to-fiber insertion losses were measured as 8.5 dB and 7.5 dB for the nanowaveguides used in the first and second FWM stages respectively.

A. First FWM Stage

The experimental setup (Fig. 1) includes two cascaded FWM stages. The first stage is used to unicast a 10-Gb/s RZ signal from the C-band to much longer wavelengths. For this stage, a 15-dBm continuous wave (CW) probe is produced by a 1312-nm laser (1312-DFB) which is amplified by a high power SOA and combined with a 10-Gb/s RZ pump using a band wavelength division multiplexer. The 17-dBm RZ pump (corresponding to ∼ 37.7-dBm peak power) is produced by a 1546.8-nm 10-GHz mode locked laser (MLL) with a 1.5-ps pulse width which is modulated by a LiNbO$_3$ Mach–Zehnder modulator (MZM) with a $2^{31}-1$ pseudo-random-bit-sequence (PRBS) from a pulsed pattern generator (PPG), and amplified by an erbium-doped fiber amplifier (EDFA). Both pump and probe are launched onto the first FWM chip to generate a 1884-nm idler. The recorded spectrum at the nanowaveguide's output (Fig. 2.a) shows a −26.8-dB conversion efficiency (defined as the idler to probe power ratio at the chip's output) in terms of average powers (corresponding to a peak-power efficiency of ∼−4.3 dB). The generated 1884-nm signal then passes through a thulium doped fiber amplifier (TDFA) and a 1900-nm isolator providing amplification as well as filtering (Fig. 2.b). We record the eye diagram and BER curve of the signal at this point using an extended-InGaAs PIN-TIA photodetector, limiting amplifier (LA), and BER-tester
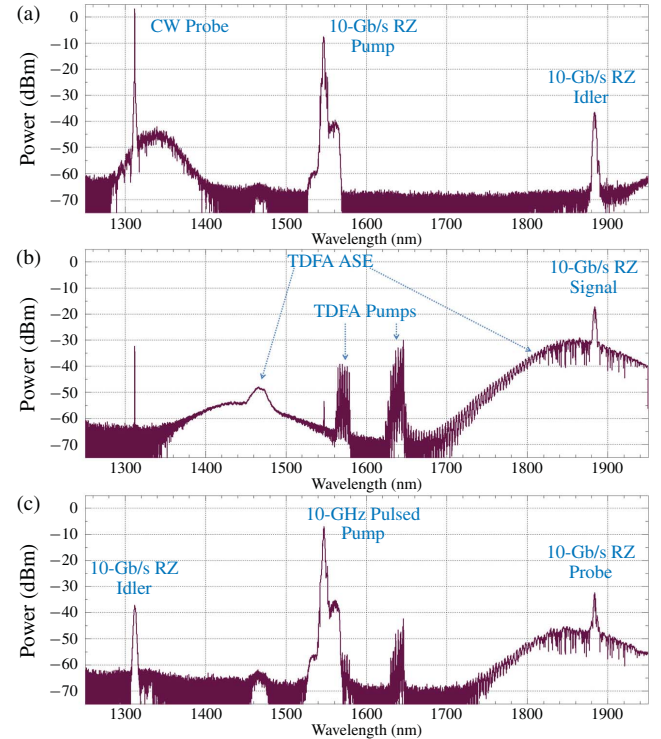
Fig. 2. Signal progression along the experiment's stages. (a) Spectrum at output of the first FWM chip with the 1312-nm CW probe, 1546.8-nm 10-Gb/s RZ pump, and generated 1884-nm 10-Gb/s RZ idler. (b) Spectrum recorded at the 1900-nm isolator's output. Beyond the amplified 1884-nm RZ signal, noise features include not fully depleted L-band TDFA pumps, TDFA asynchronous spontaneous emission (ASE) background, and not fully suppressed CW signal at 1312 nm. (c) Spectrum at the output of the second FWM chip with the 1884-nm 10-Gb/s RZ signal as the probe, the 1546.8-nm 10-GHz pulsed pump, and the generated 1312-nm 10-GB/s RZ signal.

(BERT). A variable optical attenuator (VOA) is used to vary the power incident on the detector to facilitate BER curve recording. The same receiver setup is also used to record the back-to-back case defined as the MZM output in the C-band. The photodetector sensitivity vs. wavelength is accounted for in plotting the BER curves at different wavelengths. Eye diagrams are recorded at the PIN-TIA's output using a 40-GHz digital communications analyzer (DCA). We observe open eye-diagrams on both signals and measure a power penalty of 0.4 dB as a result of the process (Fig. 3.a). Extinction-ratio improvement from the unicast operation (due to the quadratic pump-idler amplitude relation) [13] most likely negates some of the penalty from optical signal-to-noise ratio (OSNR)
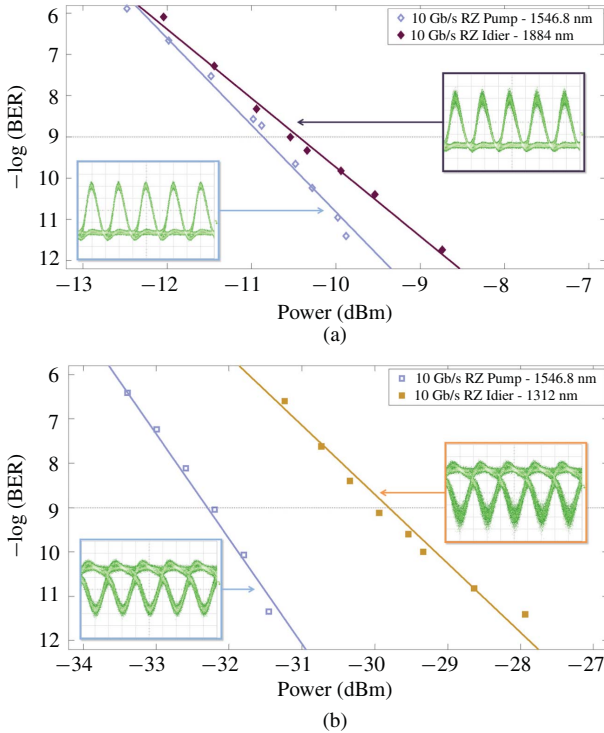
Fig. 3. (a) BER curves and eye-diagrams recorded using the extended-InGaAs PIN-TIA receiver for the 1546.8-nm pump and 1884-nm idler generated by the first FWM stage. (b) BER curves recorded using the InGaAs APD-TIA receiver for the 1546.8-nm pump and 1312-nm idler generated by the second FWM stage. The eye-diagrams were recorded from the inverted-data differential output port of the APD-TIA.

degradation from the various amplifiers and the FWM process thus resulting in this relatively low power penalty.

B. Second FWM Stage

The 1884-nm 10-Gb/s RZ signal is then combined with a non-modulated 16.5-dBm pulsed pump (34.2-dBm peak power) and both are launched into the second FWM chip to generate a 10-Gb/s RZ signal at 1312 nm. The timing of the pump with respect to the 1884-nm RZ signal is adjusted with a variable optical delay (VOD) to yield the best temporal overlap. The second stage results in a conversion efficiency of −4.8 dB (Fig. 2.c) (equal to the peak-power efficiency since both pump and probe are pulsed). The 1312-nm RZ signal then goes through a band splitter (λ) and VOA before being received by an avalanche photodiode (APD-TIA), followed by a LA and a BERT. The back-to-back case for evaluating the overall performance is measured, as before, at the MZM's output (using the APD-TIA). The overall power penalty for both FWM operations was measured to be 2.5 dB, of which 0.4 dB is accounted for by the first FWM stage with its amplification and filtering, and 2.1 dB penalty from the second FWM stage – which is mainly attributed to non-ideal suppression of the 1312-nm background signal and ASE (as seen in Fig. 2.b).

III. CONCLUSION

We have demonstrated a full FWM-based link concept for enabling telecom capabilities near the 2-μm region,

with greater than 900 nm aggregate wavelength conversion of 10-Gb/s data. Data measurements show acceptable levels of power penalty (2.5 dB) arising mainly from non-ideal filtering in the experimental setup. This demonstration is also directly extendable to higher data rates using higher symbol rate optical-time-division multiplexing (OTDM) streams.

The presented FWM-based concept of operation is enabled by the broad phase-matching bandwidth of dispersion-engineered silicon nanowaveguides, enabling effective all-optical processing across hundreds of nanometers in a single device. As silicon nanowaveguides provide continuous wavelength-conversion bandwidths exceeding 800 nm [10], [11], this scheme can potentially be adapted to provide high data rates in the whole 1.2-2 μm range, removing some of the wavelength limitations imposed by the dependence on availability of lasers, modulators, and receivers for high bit-rate communications at each wavelength band. Operation outside of the well-developed telecom bands should be able to provide a many-fold increase in optical communication links' bandwidth, assisting in scaling optical link capacity to meet future communication demands.

REFERENCES

[1] R. W. Tkach, "Scaling optical communications for the next decade and beyond," *Bell Labs Tech. J.*, vol. 14, no. 4, pp. 3–10, Feb. 2010.

[2] A. Sano, *et al.*, "69.1-Tb/s (432 × 171-Gb/s) C- and extended L-band transmission over 240 km using PDM-16-QAM modulation and digital coherent detection," in *Proc. OFC 2010*, Mar. 2010, pp. 1–3, paper PDPB7.

[3] H. Mulvad, *et al.*, "Demonstration of 5.1 Tbit/s data capacity on a single-wavelength channel," *Opt. Express*, vol. 18, no. 2, pp. 1438–1443, Jan. 2010.

[4] D. Qian, *et al.*, "101.7-Tb/s (370×294-Gb/s) PDM-128QAM-OFDM transmission over 3×55-km SSMF using pilot-based phase noise mitigation," in *Proc. NFOEC 2011*, Mar. 2011, pp. 1–3, paper PDPB5.

[5] J. Sakaguchi, *et al.*, "109-Tb/s (7×97×172-Gb/s SDM/WDM/PDM) QPSK transmission through 16.8-km homogeneous multi-core fiber," in *Proc. OFC 2011*, Mar. 2011, pp. 1–3, paper PDPB6.

[6] Y. Nishida, *et al.*, "Development of an efficient praseodymium-doped fiber amplifier," *IEEE J. Quantum Electron.*, vol. 34, no. 8, pp. 1332–1339, Aug. 1998.

[7] K. Wu, D. Ottaway, J. Munch, D. Lancaster, S. Bennetts, and S. Jackson, "Gain-switched holmium-doped fibre laser," *Opt. Express*, vol. 17, no. 23, pp. 20872–20877, Nov. 2009.

[8] B. Jalali, V. Raghunathan, D. Dimitropoulos, and O. Boyraz, "Raman-based silicon photonics," *IEEE J. Sel. Topics Quantum Electron.*, vol. 12, no. 3, pp. 412–421, May/Jun. 2006.

[9] S. Radic, C. J. McKinstrie, R. M. Jopson, J. C. Centanni, Q. Lin, and G. P. Agrawal, "Record performance of parametric amplifier constructed with highly nonlinear fibre," *Electron. Lett.*, vol. 39, no. 11, pp. 838–839, May 1, 2003.

[10] A. Turner-Foster, M. Foster, R. Salem, A. Gaeta, and M. Lipson, "Frequency conversion over two-thirds of an octave in silicon nanowaveguides," *Opt. Express*, vol. 18, no. 3, pp. 1904–1908, Feb. 2010.

[11] R. K. W. Lau, *et al.*, "Continuous-wave mid-infrared frequency conversion in silicon nanowaveguides," *Opt. Lett.*, vol. 36, no. 7, pp. 1262–1265, Apr. 2011.

[12] H. Ji, *et al.*, "Optical waveform sampling and error-free demultiplexing of 1.28 Tb/s serial data in a nanoengineered silicon waveguide," *J. Lightw. Technol.*, vol. 29, no. 4, pp. 426–431, Feb. 15, 2011.

[13] R. Salem, M. A. Foster, A. C. Turner, D. F. Geraghty, M. Lipson, and A. L. Gaeta, "Signal regeneration using low-power four-wave mixing on silicon chip," *Nature Photon.*, vol. 2, pp. 35–38, Jan. 2008.